

Inverse Dynamic Control with Outer PD Loop for Machining Robots

Ha Thanh Hai

¹Hanoi University of Industry

Corresponding Author: Ha Thanh Hai

ABSTRACT: As a machine tool, industrial robot has been researched and developed strongly due to its many technical and economic benefits. With multi-link and multi-joint structure, the robot can perform flexible motions to machining surfaces with the profiles ranging from simple to complex. However, because of a complex structure, a series of links and joints, changing of cutting forces acting on the robot, it leads to difficulties in computation of kinematics, dynamics and control of the machining robot. The article applies Denavit-Hartenberg convention, generalized coordinates, homogeneous transformation matrix, Lagrange formulation to derive kinematic and dynamic model with specific constraints on position, orientation, velocity, acceleration and forces acting on the robot during machining process. Inverse dynamic control with outer PD loop (Proportional Derivative control), based on the precise linearization method, is designed to control the motion of the machining robot. The computation results of dynamics and controls are illustrated by numerical simulation.

KEYWORDS: robot kinematics, robot dynamics, machining robot control, inverse dynamic control, milling robot, machining robot.

Date of Submission: 28-05-2022

Date of acceptance: 09-06-2022

I. INTRODUCTION

The application of serial robots which have 6 degrees of freedom for surface machining has many advantages over machine tools [1-5]. Because the machine tool with 3 axes or 3 degrees of freedom have limitation of shaping motion between the tool and the workpiece, it is difficult to machine complex surfaces. Meanwhile, machining using 6-degrees-of-freedom robot, the cutting tool is able to perform complex motions by achieving arbitrary positions and orientations in the workspace, so that the robot can machine the complex surfaces with any profile according to the technical requirements. However, the application of machining robot still faces many challenges due to the serial joint structure and the cutting forces acting on the robot during machining process [2,6]. During the cutting process, the tool is subjected to distributed cutting force at the contact position between the tool and the workpiece. The cutting force that generated in machining is a dynamic phenomenon, whose value and direction changes with time, the exact calculation of the cutting force is a difficult problem that leads to the deviation of the dynamic model. On the other hand, the shaping motion is generated from the combination of the motion of six links and six joints. Therefore, modeling and computing the dynamics of the robot is difficult and complicated.

To overcome these difficulties, there have been many research works to improve the application of robot in machining. Algorithm for kinematic computation and trajectory planning for machining robots [7]. Derivation the equations of motion, representing relationship between position, velocity, acceleration and force acting on the robot in machining process [8,9]. Considering the influence, determination and calibration of the cutting force through the differential equation of motion for the robot in milling [9], etc.

This paper presents the dynamic computation and control of a six-degree-of-freedom serial robot that is applied to mill and form surfaces (Figure 1). To derive the kinematic equations for the robot, the Denavit-Hartenberg convention and homogeneous transformation matrix are utilized. The dynamic equations of the robot are derived by applying Lagrange formulation. The derived equations of motion are convenient for programming and numerical simulation. Controller of robot based on the inverse dynamic control combined with outer PD loop is simulated to verify for intuitive and reliable results.

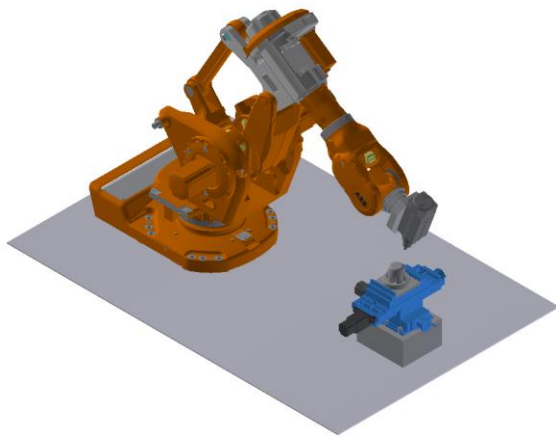


Figure 1. Serial robot with 6 degrees of freedom for machining

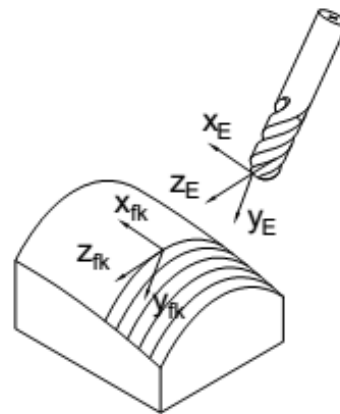


Figure 2. The coordinate frames are attached to the tool and the workpiece

II. KINEMATIC MODELING OF THE MACHINING ROBOT

1. Geometrical characteristics of the workpiece

During machining process of form-shaping surface, the tool moves along the profile and makes point contact with the surface. The machining profile is the forming curve on the surface of the workpiece. The geometry of the workpiece includes the position of the profile, the geometry of the profile and the machining surface.

Representation of the geometrical features of the robotic tool surface using the frame $x_E y_E z_E$, whose origin is at the point of contact between the tool's cutting edge and the machining surface, the axis x_E is tangent to the cutting edge, and the axis z_E is normal to the cutting edge, the frame $x_E y_E z_E$ is a right-handed frame, as shown in Figure 2.

Representation of the geometrically characteristic surface of the workpiece using the frame $x_{fk} y_{fk} z_{fk}$, whose origin is located at the point of contact between the tool and the workpiece surface on the machining profile, the axis x_{fk} is tangent to the profile, the axis z_{fk} is normal to the machining surface, the frame $x_{fk} y_{fk} z_{fk}$ is a right-handed frame, as shown in Figure 2.

Representation of the jig using the frame $x_d y_d z_d$. The workpiece is clamped on the jig. The homogeneous transformation matrix ${}^0A_{pf}$ describes the position and orientation of the machining surface with respect to the jig frame $x_d y_d z_d$. The elements of the matrix ${}^0A_{pf}$ are functions of the vector ${}^d p_f$. The vector ${}^d p_f$ represents the parameters of the generalized coordinates ${}^d x_{fk}, {}^d y_{fk}, {}^d z_{fk}, {}^d \alpha_{fk}, {}^d \beta_{fk}, {}^d \eta_{fk}$, used to describe the position and orientation of the frame $x_{fk} y_{fk} z_{fk}$ with respect to the frame $x_d y_d z_d$.

$${}^d p_f = [{}^d x_{fk}, {}^d y_{fk}, {}^d z_{fk}, {}^d \alpha_{fk}, {}^d \beta_{fk}, {}^d \eta_{fk}]^T \tag{1}$$

$${}^d A_{pf} = {}^d A_f({}^d p_f) = \begin{bmatrix} {}^d C_f({}^d p_f) & {}^d r_f({}^d p_f) \\ 0^T & 1 \end{bmatrix} \tag{2}$$

The homogeneous transformation matrix ${}^d A_{pE}$ describes the position and orientation of the cutting tool with respect to the jig frame as a function of the vector ${}^d p_E$. The vector ${}^d p_E$ represents the parameters of the generalized coordinates ${}^d x_E, {}^d y_E, {}^d z_E, {}^d \alpha_E, {}^d \beta_E, {}^d \eta_E$, used to describe the position and orientation of the frame $x_E y_E z_E$ with respect to the frame $x_d y_d z_d$.

$${}^d p_E = [p_1, p_2, \dots, p_6]^T = [{}^d x_E, {}^d y_E, {}^d z_E, {}^d \alpha_E, {}^d \beta_E, {}^d \eta_E]^T \tag{3}$$

$${}^d A_{pE} = {}^d A_E({}^d p_E) = \begin{bmatrix} {}^d C_E({}^d p_E) & {}^d r_E({}^d p_E) \\ 0^T & 1 \end{bmatrix} \tag{4}$$

The condition for the cutting tool to shape the workpiece surface is that the tool frame $x_E y_E z_E$ coincides with the workpiece frame $x_{fk} y_{fk} z_{fk}$. So from (3) and (4) get (5).

$${}^d A_{pE} = {}^d A_{pf} \tag{5}$$

2. Representation of the tool in machining process

Each link of the robot is represented by a coordinate frame, according to the Denavit-Hartenberg convention: a fixed coordinate frame $x_0 y_0 z_0$ is placed on the base of the robot. The $x_i y_i z_i$ frame ($i=1, \dots, 6$) is attached to the link i , respectively, as shown in Figure 3.

The Denavit-Hartenberg parameters of the robot are specified in Table 1.

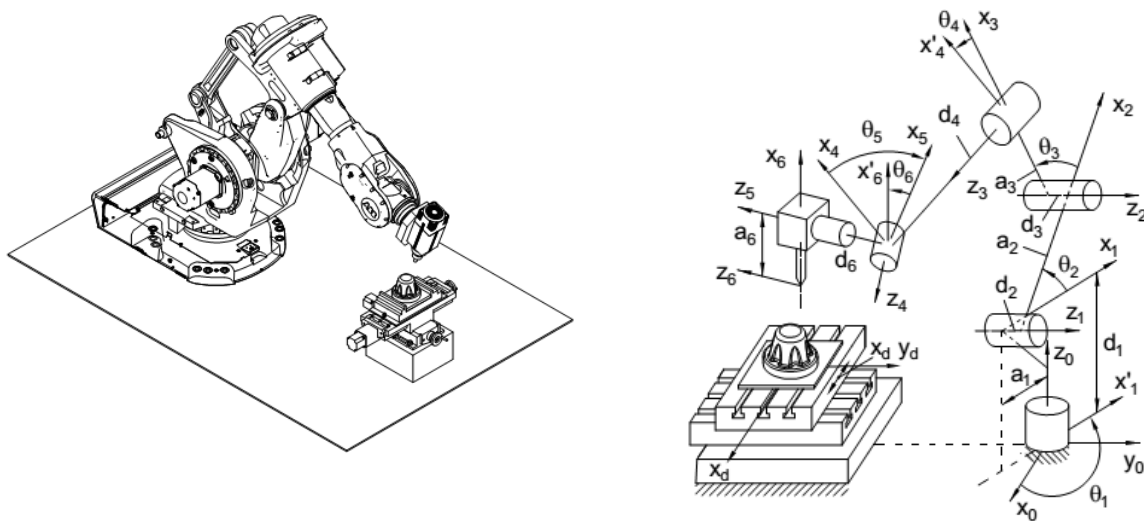


Figure 3. The machining robot

Table 1. Denavit-Hartenberg parameters of the robot

Links -Joint	θ_i (degree)	d_i (mm)	a_i (mm)	α_i (rad)
1	θ_1	$d_1 = 514,5$	$a_1 = 300$	$\pi/2$
2	θ_2	0	$a_2 = 700$	0
3	θ_3	0	$a_3 = 280$	$-\pi/2$
4	θ_4	$d_4 = 1060,24$	0	$\pi/2$
5	θ_5	0	0	$-\pi/2$
6	θ_6	$d_6 = 377$	$a_6 = -256$	0

The Denavit-Hartenberg homogeneous transformation matrix ${}^{i-1}A_i$ ($i=1,\dots,6$) describes the position and orientation of link i with respect to the link $i - 1$.

$${}^{i-1}A_i = \begin{bmatrix} {}^{i-1}C_i(\theta_i) & d_i r_i(\theta_i) \\ 0^T & 1 \end{bmatrix} \tag{6}$$

The joint coordinate vector is represented by (7).

$$q = [q_1, q_2, \dots, q_6]^T = [\theta_1, \theta_2, \dots, \theta_6]^T \tag{7}$$

The homogeneous transformation matrix 0A_i ($i=1,\dots,6$) describes the position and orientation of link i with respect to the base frame of the robot.

$${}^0A_i = {}^0A_1 {}^1A_2 \dots {}^{i-1}A_i = \begin{bmatrix} {}^0C_i(q) & {}^0r_i(q) \\ 0^T & 1 \end{bmatrix} \tag{8}$$

The homogenous transformation matrix 6A_E describes the position and orientation of the tool with respect to the last link of the robot (Link 6). The elements of the matrix 6A_E are functions of the kinematics parameters ${}^6x_E, {}^6y_E, {}^6z_E, {}^6\alpha_E, {}^6\beta_E, {}^6\eta_E$. These kinematic parameters are used to describe the position and orientation of the frame $x_E y_E z_E$ with respect to the frame $x_6 y_6 z_6$, Table 2. 6A_E is a constant matrix and is represented by (9).

Table 2. Kinematic parameters of the tool with respect to the frame $x_6 y_6 z_6$

6x_E (mm)	6y_E (mm)	6z_E (mm)	${}^6\alpha_E$ (rad)	${}^6\beta_E$ (rad)	${}^6\eta_E$ (rad)
0	0	0	π	$\pi/2$	0

$${}^6A_E = \begin{bmatrix} {}^6C_E & {}^6r_E \\ 0^T & 1 \end{bmatrix} \tag{9}$$

The homogenous transformation matrix 0A_E determines the position and orientation of the tool frame with respect to the base frame according to the robot-tool kinematics transmission chain.

$${}^0A_E = {}^0A_1 {}^1A_2 \dots {}^5A_6 {}^6A_E \tag{10}$$

The homogenous transformation matrix 0A_d determines the position and orientation of the jig with respect to the base frame. The matrix 0A_d is created by kinematic parameters ${}^0x_d, {}^0y_d, {}^0z_d, {}^0\alpha_d, {}^0\beta_d, {}^0\eta_d$. Table 3 shows the kinematic parameters ${}^0x_d, {}^0y_d, {}^0z_d, {}^0\alpha_d, {}^0\beta_d, {}^0\eta_d$.

Table 3. Kinematic parameters of the jig with respect to the frame $x_0y_0z_0$

0x_d (mm)	0y_d (mm)	0z_d (mm)	${}^0\alpha_d$ (rad)	${}^0\beta_d$ (rad)	${}^0\eta_d$ (rad)
0	-1361	196,6	0	0	0

$${}^0A_d = \begin{bmatrix} {}^0C_d & {}^0r_d \\ 0^T & 1 \end{bmatrix} \tag{11}$$

The homogeneous transformation matrix 0A_E describes the position and orientation of the tool with respect to the base frame according to the jig - tool kinematics transmission chain.

$${}^0A_E = {}^0A_d {}^dA_E \tag{12}$$

3. Direct kinematics of the machining robot

Equalizing the sides of (10) and (12) and get (13)

$${}^dA_E = {}^dA_E ({}^dP_E) = {}^0A_d^{-1} {}^0A_1 {}^1A_2 \dots {}^5A_6 {}^6A_E = \begin{bmatrix} {}^dC_E(q) & {}^dR_E(q) \\ 0^T & 1 \end{bmatrix} \tag{13}$$

In the process of machining part surface by robot, the position q , velocity \dot{q} , acceleration \ddot{q} of the joint is measured by the controller via the encoders attached to the joints. From equation (13) and derivatives of (13), position and orientation dP_E , velocity ${}^d\dot{P}_E$, acceleration ${}^d\ddot{P}_E$ are determined and expressed in (14).

$${}^dP_E = [p_1, p_2, \dots, p_6]^T; \quad {}^d\dot{P}_E = [\dot{p}_1, \dot{p}_2, \dots, \dot{p}_6]^T; \quad {}^d\ddot{P}_E = [\ddot{p}_1, \ddot{p}_2, \dots, \ddot{p}_6]^T \tag{14}$$

4. Inverse kinematics of the machining robot

Equalizing both sides of (4) and (13) to get equation (15)

$$\begin{bmatrix} {}^dC_E(q) & {}^dR_E(q) \\ 0^T & 1 \end{bmatrix} = \begin{bmatrix} {}^dC_E({}^dP_E) & {}^dR_E({}^dP_E) \\ 0^T & 1 \end{bmatrix} \tag{15}$$

Equalizing the components of both sides of the equation (15) to get kinematics equations (16)

$$\begin{cases} f_1 = {}^dC_{11}(q) - {}^dC_{11}({}^dP_E) = 0 \\ f_2 = {}^dC_{22}(q) - {}^dC_{22}({}^dP_E) = 0 \\ f_3 = {}^dC_{33}(q) - {}^dC_{33}({}^dP_E) = 0 \\ f_4 = {}^dX_E(q) - {}^dX_E({}^dP_E) = 0 \\ f_5 = {}^dY_E(q) - {}^dY_E({}^dP_E) = 0 \\ f_6 = {}^dZ_E(q) - {}^dZ_E({}^dP_E) = 0 \end{cases} \tag{16}$$

In (16), the first three equations represent the relationship of orientation, the following three equations represent the relationship of position of the tool frame with respect to the jig frame. To perform the machining process, the tool moves along the machining profile, which is the motion of the tool frame $x_Ey_Ez_E$ between consecutive points on the profile so that at each machining time the frame $x_Ey_Ez_E$ coincides with the frame $x_fy_fz_f$. According to the machining technology requirements for forming part surface, the position and orientation vector dP_E , velocity vector ${}^d\dot{P}_E$, acceleration vector ${}^d\ddot{P}_E$ of the tool along the machining profile is a determined function of time. From (16) and derivatives of (16), the position q , velocity \dot{q} , acceleration \ddot{q} of the joint can be determined and expressed in (17).

$$q = [q_1, q_2, \dots, q_6]^T; \quad \dot{q} = [\dot{q}_1, \dot{q}_2, \dots, \dot{q}_6]^T; \quad \ddot{q} = [\ddot{q}_1, \ddot{q}_2, \dots, \ddot{q}_6]^T \tag{17}$$

III. MACHINING ROBOT DYNAMICS

The dynamic parameters of the machining robot are shown in Table 4.

Table 4. Dynamic parameters of the machining robot

TT	Center of gravity position, in the joint frame (mm)			Mass (kg)	Inertial moment of the links with respect to the frame attaching at the center of mass (kg.mm ²)					
	x_{Ci}	y_{Ci}	z_{Ci}		I_{xx}	I_{yy}	I_{zz}	I_{xy}	I_{yz}	I_{zx}
1	101,27	-161,53	17,51	979,776	107464105,56	106997584,679	76391174,876	-15737765,26	1079510,623	2528210,401
2	-389,98	57,61	15,15	255,520	3908083,112	12110291,517	11739707,489	-454581,588	110524,194	877218,740
3	-70,78	-52,67	-194,76	356,302	15150531,425	15511051,346	10981064,424	-843859,157	109739,085	349159,306
4	0	-344,49	-14,39	268,237	25403793,206	3355342,987	23996196,983	-13888,740	1000831,563	9449,097
5	0	40,29	1,05	55,235	465398,004	441427,864	231978,283	70,639	9848,368	19,282
6	290,94	40,29	-64,09	36,306	305737,658	512275,019	383507,486	-92,536	-36,246	-41461,026

Adopting Lagrange formulation, the equations of motion of the machining robot is shown in (18)

$$M(q)\ddot{q} + C(q,\dot{q}) + G(q) + Q = U \tag{18}$$

The components in equation (18) are determined from the following expressions:

$$M(q) = \left[\sum_{i=1}^6 (J_{Ti}^T m_i J_{Ti} + J_{Ri}^T \Theta_{ci} J_{Ri}) \right]_{(6 \times 6)}; \quad J_{Ti} = \frac{\partial r_i}{\partial q}; \quad J_{Ri} = \frac{\partial \omega_i}{\partial \dot{q}} \tag{19}$$

(19) represents the generalized mass matrix $M(q)$. In which, m_i denotes mass of link i , J_{Ti} denotes the translational Jacobian matrix; J_{Ri} denotes the rotating Jacobian matrix; Θ_{ci} denotes inertial matrix of link i with respect to the frame that attached to its center of mass.

$$C(q, \dot{q}) = [c_j(q, \dot{q})]_{(6 \times 1)}; c_j(q, \dot{q}) = \frac{1}{2} \sum_{k,l=1}^6 \left(\frac{\partial m_{kl}}{\partial q_l} + \frac{\partial m_{lj}}{\partial q_k} - \frac{\partial m_{kl}}{\partial q_j} \right) \dot{q}_k \dot{q}_l \quad (20)$$

$C(q, \dot{q})$ is the generalized force vector of Coriolis and centrifugal forces. In which, m_{kl} ($k, l = 1, \dots, 6$) are the components of the matrix $M(q)$.

$$G(q) = [g_j(q)]_{(6 \times 1)}; g_j(q) = \frac{\partial \Pi}{\partial q_j} \quad (21)$$

Equation (21) represents the generalized force vector of potential forces. Π denotes the potential energy of the system.

$$U = [u_j]_{(6 \times 1)}; u_j = \tau_j \quad (22)$$

U denotes the generalized force vector of the driving forces. τ_i denotes the driving force at the joints of the robot.

$$Q = [Q_j]_{(6 \times 1)} = J_{TE}^T F + J_{RE}^T M; \quad J_{TE} = \frac{\partial r_E}{\partial q}; J_{RE} = \frac{\partial \omega_E}{\partial \dot{q}}; F = [F_x, F_y, F_z]^T; M = [M_x, M_y, M_z]^T \quad (23)$$

Expression (23) represents the generalized force vector Q of the none potential force that is the cutting force F and the cutting torque M acting on the tool during machining process. The cutting force and cutting torque greatly affect the motion of the robot when machining and shaping the surface of the part. In (23), J_{TE} denotes the translational Jacobian matrix; J_{RE} denotes the rotating Jacobian matrix; with z teeth are involved in cutting at the same time, the cutting force in the x, y, z directions is F_x, F_y, F_z , respectively, calculated in (34) [10-15].

$$F_x = \sum_{i=1}^z \left(\int_{z_{j1}}^{z_{j2}} dF_{xi} dz \right); F_y = \sum_{i=1}^z \left(\int_{z_{j1}}^{z_{j2}} dF_{yi} dz \right); F_z = \sum_{i=1}^z \left(\int_{z_{j1}}^{z_{j2}} dF_{zi} dz \right) \quad (24)$$

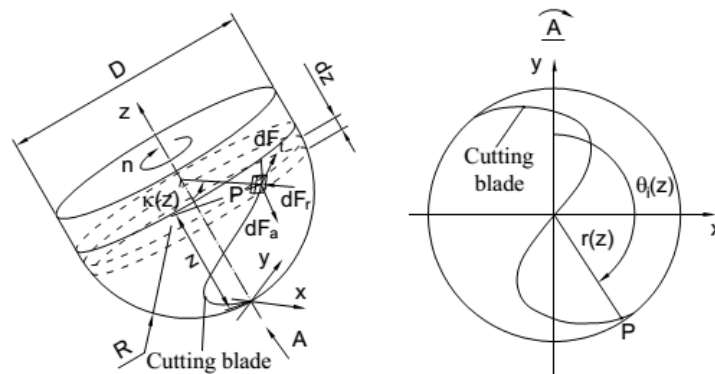


Figure 4. Model of cutting force of end mills in milling

The elemental cutting force $dF_{xi}, dF_{yi}, dF_{zi}$ in the direction of x, y, z axes acts on the element area P of the cutting edge i of the end mills. z_{j1}, z_{j2} are the lower and upper limits of the area element of tooth i .

$$dF = [dF_{xi}, dF_{yi}, dF_{zi}]^T = {}^{xyz}C_{tra} [dF_{ti}, dF_{ri}, dF_{ai}]^T \quad (25)$$

$dF_{ti}, dF_{ri}, dF_{ai}$ denote cutting forces acting on the blade element i in the tangent (t), radial (r) and axial (a) directions, respectively; Matrix ${}^{xyz}C_{tra}$ converts force element from direction t, r, a to direction x, y, z .

$$dF_{ui} = K_{uc} a_i db + K_{ue} dS; u = (t, r, a) \quad (26)$$

In (26), K_{uc} and K_{ue} denote the coefficient of cutting forces in the u direction, respectively; db denotes cutting element length in the direction along the cutting velocity; a_i denotes cutting thickness due to tooth element i in machining; dS denotes the element length of the tooth section i of a helical cut.

IV. INVERSE DYNAMIC CONTROL WITH OUTER PD LOOP FOR MACHINING ROBOTS

From the dynamic equation (18), choose the control law as follows:

$$U = \alpha u + \beta \quad (27)$$

In which, U denotes control force.

$$\alpha = M(q); \beta = C(q, \dot{q}) + G(q) + Q \quad (28)$$

$$u = \ddot{q}_d + K_p \dot{e} + K_{pe} \quad (29)$$

The matrices of the proportional and derivative coefficients K_p, K_D are calculated according to (30),

$$K_p = \text{diag}\{K_{p1}, K_{p2}, \dots, K_{p6}\}; K_{pi} > 0 \quad i = 1, 2, \dots, 6 \quad (30)$$

$$K_D = \text{diag}\{K_{D1}, K_{D2}, \dots, K_{D6}\}; K_{Di} > 0 \quad i = 1, 2, \dots, 6 \tag{31}$$

The position and velocity deviations of the robot joints are determined according to (32), (33)

$$e = [e_1, e_2, \dots, e_6]^T; e = q_d - q \tag{32}$$

$$\dot{e} = [\dot{e}_1, \dot{e}_2, \dots, \dot{e}_6]^T; \dot{e} = \dot{q}_d - \dot{q} \tag{33}$$

The set values of the joint variables and its first, second derivatives are $q_d, \dot{q}_d, \ddot{q}_d$. These values are determined from the computing results of the motion trajectory of the inverse dynamic problem.

The real values of the joint variables and its first, second derivatives are q, \dot{q}, \ddot{q} .

The controller model is depicted in Fig 5.

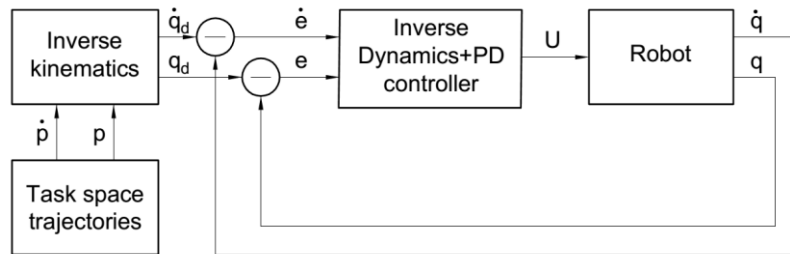


Figure 5. Block scheme of the inverse dynamic control with outer PD loop

V. COMPUTING INVERSE KINEMATICS AND CONTROL THE MACHINING ROBOT

1. Parameters

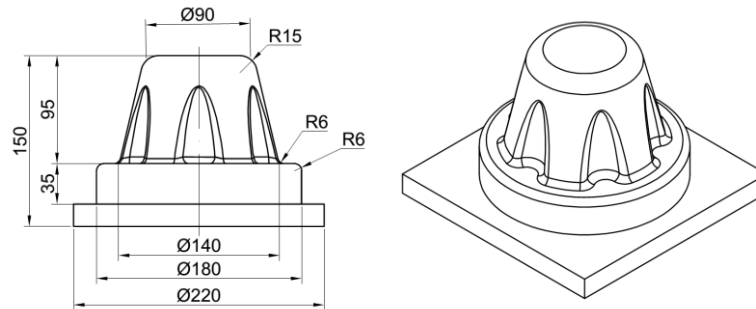
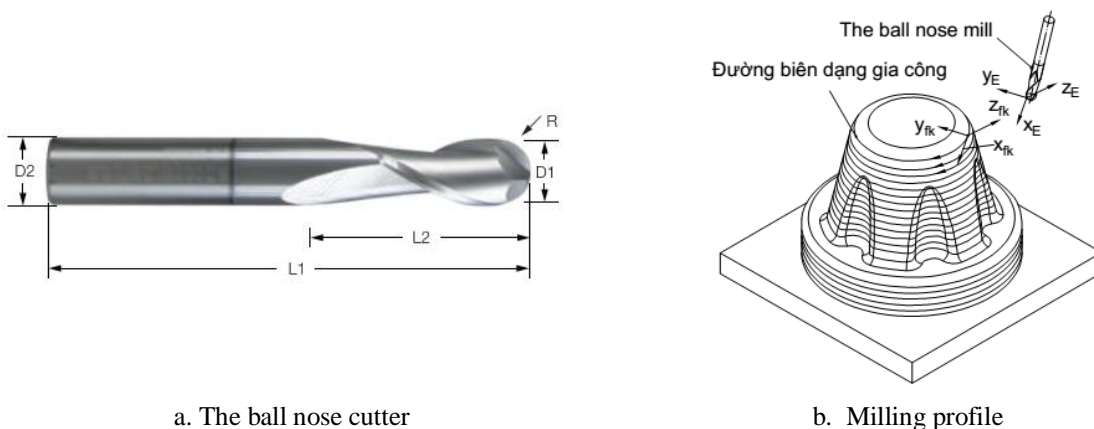


Figure 6. The part

This paper presents an example using a robot milling a part surface. The workpiece is made of titanium alloy Ti₆Al₄V, with dimensions and shapes as shown in Figure 6. The tool is a carbide end mill with 2 helical teeth, 8mm in diameter shown in Figure 7a. The displacement trajectory of the cutter at each machining time on the profile C is shown in Figure 7b. The machining profile C is calculated and saved as a data file for use in dynamic computation and control of the robot.



a. The ball nose cutter

b. Milling profile

Figure 7. Ball end mills and machining trajectory

Using a milling robot to shape the part surface with the parameters of the ball nose mill and the milling process shown in Table 5. In which n is the number of revolutions of the end mill; S feed amount, h₀ depth of cut.

Table 5. Parameters of ball nose cutter and milling process

Cutter's material	D ₁ (mm)	D ₂ (mm)	L ₁ (mm)	L ₂ (mm)	Z (răng)	n (vg/ph)	S _z (mm/răng)	h ₀ (mm)	Cooling liquor
Carbide	8	8	63	20	2	4000	0,1	0,2	Emunxi

The cutting force in milling is calculated according to the formula (24), (25), (26) with the values of the cutting force coefficient (in Table 5) corresponding to the selected cutting mode according to reference [16]. The calculation results of the cutting force, and the cutting torque in milling are shown in Figure 8. The values of the cutting torques M_x, M_y, M_z are very small, so they should be ignored.

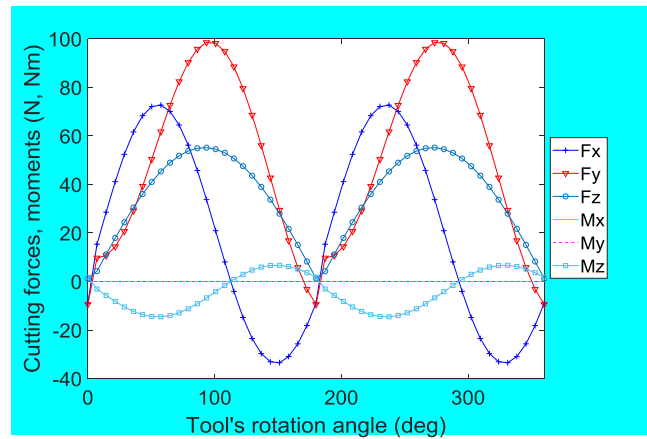


Figure 8. Cutting forces in milling

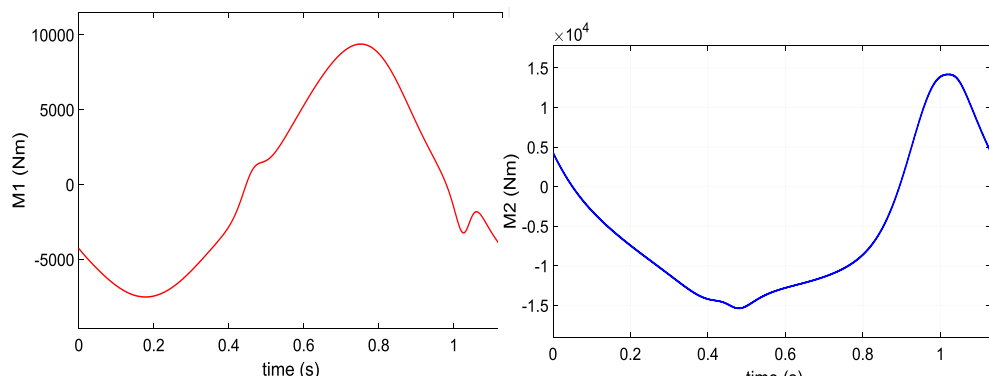
The values of K_P, K_D are chosen as follows:

$$K_P = \text{diag}\{6400, 6400, \dots, 6400\} \tag{34}$$

$$K_D = \text{diag}\{160, 160, \dots, 160\} \tag{35}$$

2. Computation and simulation results

The robot is applied to mill the part surface. With the given data, computed position q, velocity q̇, acceleration q̈ of the robot joints, thereby solving the dynamics problem and computed the driving torque at the robot joints in Figure 9.



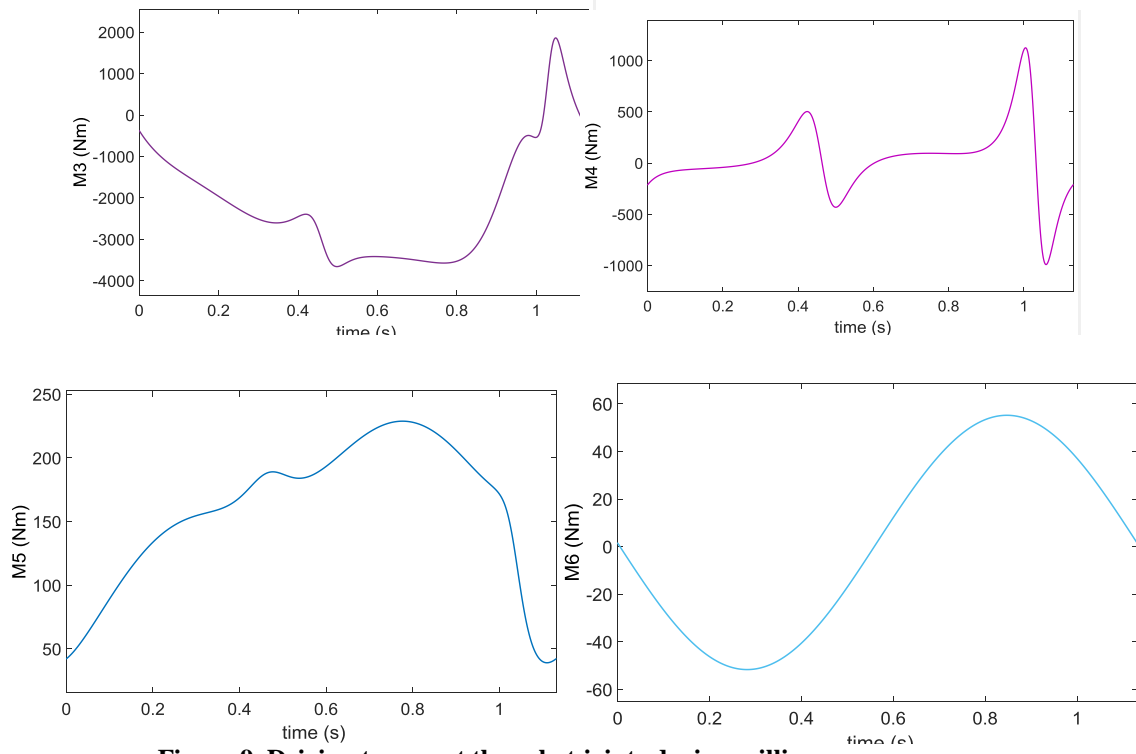
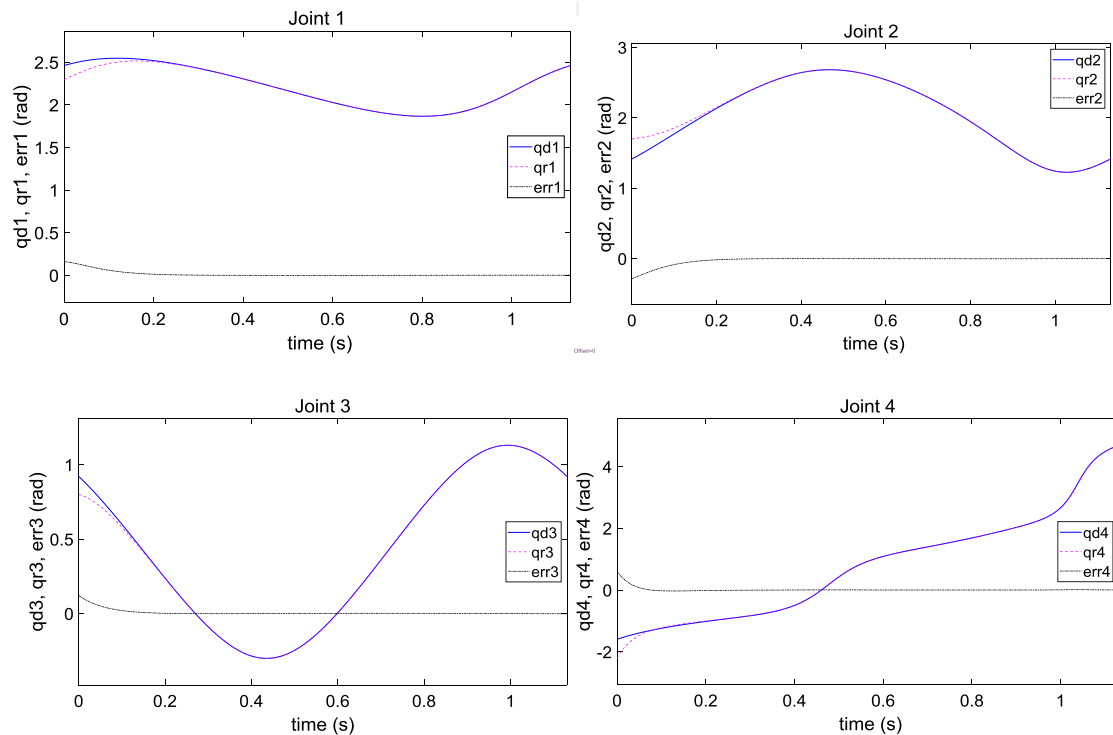


Figure 9. Driving torque at the robot joints during milling process

The motion law of robot joints obtained from the simulation program of inverse dynamic control with outer PD loop for the part surface milling is shown in Figure 10.



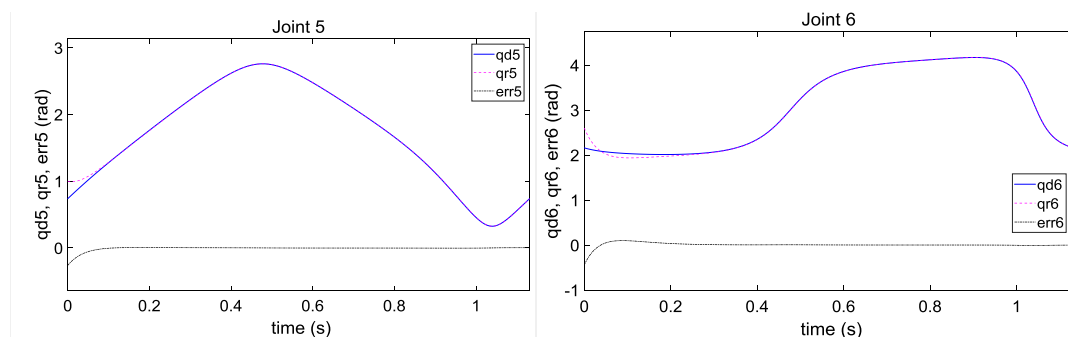


Figure 10. Control results in the joint space

Figure 10 shows that the initial position of the joints converges to the time setting values below 0.2s, the error is 0.0001 rad (very small static deviation). The robot milling the part surface is controlled to match the desired trajectory with high accuracy.

VI. CONCLUSION

The simulation results show the following conclusions:

Serial structural robot is researched, surveyed and calculated to match the requirements of milling and shaping technology for surfaces with different configurations.

From the motion planning of machining robots, it is possible to build flexible computation and programming programs when machining and milling of part surfaces with profiles from simple to complex.

Applying the Denevit-Hartenberg convention, generalized coordinates, homogeneous transformation matrix, Lagrange formulation allows convenient computation and programming to derive and solve the equations of kinematics, dynamics and control machining robot. The inverse dynamic control with outer PD loop, based on the precise linearization method is designed to meet the requirements of precision in machining.

The numerical simulation results of dynamics and inverse dynamic control with outer PD loop confirm the reliability of the proposed method.

REFERENCES

- [1]. Appleton E, Williams DJ - *Industrial robot applications*. HALSTED PRESS, New York (1987), 229 pages.
- [2]. Wei Ji, Lihui Wang: *Industrial robotic Machining: A review*, The International Journal of Advanced manufacturing Technology. September 2011, pp. 1-17.
- [3]. John Pandremenos, Christos Doukas, Panagiotis Stavropoulos, George Chryssolouris-*Machining with robots: a critical review*. Proceedings of DET2011 7th International Conference on Digital Enterprise Technology, Athens, Greece, 28-30 September 2011.
- [4]. Maciej Petko, Konrad Gac, Grzegorz Góra, Grzegorz Karpiel, Janusz Ochoński, Konrad Kobus: *CNC system of the 5-axis hybrid robot for milling*. Mechatronics, Vol. 37, Aug. 2016, pp. 89-99.
- [5]. Iglesias I, Sebastián M A, Aresc J E - *Overview of the state of robotic machining: Current situation and future potential*. ScienceDirect, Procedia Engineering 132 (2015) 911 – 917.
- [6]. Maciej Petko, Grzegorz Karpiel, Konrad Gac, Grzegorz Góra, Konrad Kobus, Janusz Ochoński: *Trajectory tracking controller of the hybrid robot for milling*. Mechatronics, Vol. 37, Aug. 2016, pp. 100-111.
- [7]. Phan Bui Khoi, Ha Thanh Hai. *Investigation of kinematics and motion planning for mechanical machining robots*. Proceedings of the National Conference of Engineering Mechanics, Vol. 2, (2015), pp. 407-418 (In Vietnamese).
- [8]. Phan Bui Khoi, Ha Thanh Hai. *Robot dynamics in mechanical processing*. Proceedings of the National Conference of Engineering Mechanics, Vol. 2, (2015), pp. 419-427 (In Vietnamese).
- [9]. Phan Bui Khoi, Ha Thanh Hai. *Force analysis of a robot in machining process*. Proceeding of National conference on machines and mechanisms, (2015), pp. 346-359
- [10]. Ferrusquía, A.; Yu, W.; Soria, A. Position/force control of robot manipulators using reinforcement learning. *Ind. Robot Int. J. Robot. Res. Appl.* **2019**, *46*, 267–280.
- [11]. Lacerda, H.B.; Lima, V.T. Evaluation of cutting forces and prediction of chatter vibrations in milling. *J. Braz. Soc. Mech. Sci. Eng.* **2004**, *26*, 74–81.
- [12]. Leonesio, M.; Villagrossi, E.; Beschi, M.; Marini, A.; Bianchi, G.; Pedrocchi, N.; Isaev, A. Vibration analysis of robotic milling tasks. *Procedia Cirp* **2018**, *67*, 262–267.
- [13]. Wang, G.; Dong, H.; Guo, Y.; Ke, Y. Dynamic cutting force modeling and experimental study of industrial robotic boring. *Int. J. Adv. Manuf. Technol.* **2016**, *86*, 179–190.
- [14]. Lazoglu, I. A new identification method of specific cutting coefficients for ball end milling. *Procedia Cirp* **2014**, *14*, 182–187.
- [15]. Ghorbani, H.; Moetakef-Imani, B. Specific cutting force and cutting condition interaction modeling for round insert face milling operation. *Int. J. Adv. Manuf. Technol.* **2016**, *84*, 1705–1715.
- [16]. Gradišek, Janez, Martin Kalveram, and Klaus Weinert. "Mechanistic identification of specific force coefficients for a general end mill." *International Journal of Machine Tools and Manufacture* 44.4 (2004): 401-414.